2017

Effects of vitrectomy and lensectomy on older rhesus macaques: Oxygen distribution, antioxidant status, and aqueous humor dynamics

Carla J. Siegried
Washington University School of Medicine in St. Louis

Ying-Bo Shui
Washington University School of Medicine in St. Louis

Baohe Tian
University of Wisconsin-Madison

Michael Nork
University of Wisconsin-Madison

Gregg A. Heatley
University of Wisconsin-Madison

See next page for additional authors

Effects of Vitrectomy and Lensectomy on Older Rhesus Macaques: Oxygen Distribution, Antioxidant Status, and Aqueous Humor Dynamics

Carla J. Siegfried,[1] Ying-Bo Shui,[1] Baohe Tian,[2] T. Michael Nork,[2] Gregg A. Heatley,[2] and Paul L. Kaufman[2]

[1]Department of Ophthalmology and Visual Sciences, Washington University School of Medicine, St. Louis, Missouri, United States
[2]Department of Ophthalmology & Visual Sciences, School of Medicine & Public Health, University of Wisconsin-Madison, Madison, Wisconsin, United States

Correspondence: Carla J. Siegfried, Washington University Department of Ophthalmology and Visual Sciences, 660 South Euclid Avenue, Campus Box 8096, St. Louis, MO 63110, USA; siegfried@wustl.edu.

Submitted: March 18, 2017
Accepted: June 24, 2017

Citation: Siegfried CJ, Shui Y-B, Tian B, Nork TM, Heatley GA, Kaufman PL. Effects of vitrectomy and lensectomy on older rhesus macaques: oxygen distribution, antioxidant status, and aqueous humor dynamics. *Invest Ophthalmol Vis Sci*. 2017;58:4003–4014. DOI:10.1167/iovs.17-21890

Purpose. The purpose of this study is to evaluate effects of vitrectomy (PPV) and lens extraction with intraocular lens implantation (PE/IOL) on molecular oxygen (pO_2) distribution, aqueous humor antioxidant–oxidant balance, aqueous humor dynamics, and histopathologic changes in the trabecular meshwork (TM) in the older macaque monkey.

Methods. Six rhesus monkeys underwent PPV followed by PE/IOL. pO_2, outflow facility, and intraocular pressure (IOP) were measured. Aqueous and vitreous humor specimens were analyzed for antioxidant status and 8-hydroxy-2′-deoxyguanosine (8-OHdG), a marker of oxidative damage. TM specimens were obtained for immunohistochemical and quantitative PCR analysis.

Results. pO_2 at baseline revealed steep gradients in the anterior chamber and low levels in the posterior chamber (PC) and around the lens. Following PPV and PE/IOL, pO_2 significantly increased in the PC, around the IOL, and angle. IOP increased following both surgical interventions, with no change in outflow facility. Histopathologic analysis did not show changes in TM cell quantification, but there was an increase in 8-OHdG. Quantitative PCR did not reveal significant differences in glaucoma-related gene expression. Aqueous and vitreous humor analysis revealed decreased ascorbate and total reactive antioxidant potential and increased 8-OHdG in the aqueous humor only in the surgical eyes.

Conclusions. Oxygen distribution in the older rhesus monkey is similar to humans at baseline and following surgical interventions. Our findings of histopathologic changes of TM oxidative damage and alterations in the oxidant-antioxidant balance suggest a potential correlation of increased oxygen exposure with oxidative stress/damage and the development of open angle glaucoma.

Keywords: oxidative damage, trabecular meshwork, glaucoma

Modern pars plana vitrectomy procedures, first developed by Machemer in 1969,[1] are currently used for a variety of vitreoretinal pathologies, including macular hole repair, rhegmatogenous retinal detachment repair, vitreous hemorrhage removal, epiretinal membrane removal, and, most recently, removal of bothersome vitreous floaters.[2] The increased utilization of these procedures reflects the safety profile of modern techniques and the successful outcomes in these potentially disabling conditions.[3,4] In these cases, the occurrence of postvitrectomy nuclear sclerotic cataract formation is increased.[5–10] Few prospective studies have been performed to evaluate this finding, frequently requiring cataract extraction within 24 months in 37% to 95% of individuals. This rapid development of nuclear sclerosis is associated with increased oxygen levels in the vitreous cavity and surrounding the lens, which normally exists in a relatively hypoxic environment.[11] These findings led to our group's proposal that this increased exposure to oxygen leads to oxidative lens damage and subsequent nuclear cataract formation. Notably, gauge size of the vitrector did not affect the development of cataract,[12] but older age, myopia, and increased vitreous liquefaction[13] do increase this risk.

Additionally, several studies have demonstrated increased risk of ocular hypertension and/or open angle glaucoma development following these consecutive procedures,[14–18] and we are investigating Chang's hypothesis that increased oxygen in the anterior segment may contribute to oxidative damage to the trabecular meshwork.[19] Other retrospective studies have not supported these findings within limited follow-up periods,[20–22] and a prospective trial[23] is underway to provide further information on this risk factor for the most common cause of irreversible blindness. The trabecular meshwork (TM) tissue provides the pathway, and resistance, for the conventional outflow of aqueous humor from the anterior chamber (AC). Alterations in this outflow pathway may lead to elevation of intraocular pressure (IOP) and the development of glaucoma. Our previous studies demonstrated changes in the tightly controlled intraocular oxygen gradients in human subjects undergoing pars plana vitrectomy (PPV) and subsequent cataract extraction.[24]

In this study, the older rhesus macaque monkey provides an opportunity to study specific effects of increased oxygen levels in the anterior and posterior segments of the eye following vitrectomy and subsequent lens extraction, on IOP, aqueous humor outflow facility, TM histopathology, and markers of oxidative damage and antioxidant status in the ocular fluids.

Methods

Study Design

The University of Wisconsin Animal Care and Use Committee approved the protocol, adhering to the ARVO Statement for the Use of Animals in Ophthalmic and Vision Research. This prospective, cross-sectional study was designed to evaluate the effects of PPV followed by phacoemulsification lens extraction and posterior chamber intraocular lens implantation (PE/IOL) on intraocular oxygen levels, as well as functional and histologic alterations of the TM.

Animals

Six rhesus monkeys (*Macaca mulatta*), age 20 to 25 years, weighing at least 6 kg with bilateral normal ocular examinations by biomicroscopy and tonometry, were screened and trained for the study. The monkeys were housed in the Wisconsin National Primate Research Center at the Wisconsin Institutes for Medical Research complex, and all experiments were done in accordance with the ARVO Statement for the Use of Animals in Ophthalmic and Vision Research. After the monkeys were acclimated to the facility and trained to receive topical treatments consciously, the experiments were initiated as described below. Monkeys were anesthetized with intramuscular (IM) ketamine (10 to 20 mg/kg initial), followed by intravenous pentobarbital anesthesia (8 to 15 mg/kg initial; 5 to 10 mg/kg supplemental) for the perfusion outflow facility studies and endotracheal inhalation isofluorane anesthesia for the surgical interventions. For the pneumatography studies, 0.2 mg/kg IM midazolam plus 0.04 mg/kg IM atropine was administered. During surgery, animals received systemic monitoring including heart rate, respiration rate and/or end-tidal CO_2, SpO_2, temperature, and blood pressure. During our measurements of intraocular oxygen, special efforts were made to decrease FiO_2 to approach 21% (room air levels), with maintenance of peripheral blood saturation (SaO_2) to baseline levels of 93% to 97%. Following each ocular surgery, the eye received subconjunctival injections of gentamycin and methylprednisolone acetate, followed by administration of polymixin/neomycin/bacitracin antibiotic ointment into the conjunctival sac. In cases of persistent inflammation, 1% atropine ointment was also applied to the eye. Postprocedure analgesia with buprenorphine (0.005 to 0.02 mg/kg IM at 6- to 12-hour intervals) or carprofen in multimodal analgesia where animals received buprenorphine (0.005 to 0.02 mg/kg IM at intervals of not more than 20 hours) and carprofen (2 to 4 mg/kg orally, intravenous, subcutaneous, or IM), butorphanol (0.05 to 0.2 mg/kg IM at 2- to 4-hour intervals), meloxicam (0.1 to 0.2 mg/kg orally), and/or flunixin meglumine (1 to 2 mg/kg, 1 to 2 times daily IM) was administered for up to 3 days following all surgical procedures, and/or at any other time deemed necessary by the principal investigator, the collaborators at the UW, or attending veterinary staff. The analgesia dosing was chosen depending on the animal's signs of pain (e.g., squinting, swollen eyelids, rubbing of the eyes, or tearing). The surgical and sham-operated eyes were observed by the research staff during daily treatment (including topical 1% tropicamide and 10% phenylephrine) for 2 weeks to monitor surgical recovery.

Baseline Measurements

Slit-lamp biomicroscopy (SLE), corneal pachymetry (Pachmate; DGH Technology, Exton, PA, USA; average of three readings), fundus photography, and outflow facility measurements by pneumatonography were performed at least 6 weeks prior to each surgical intervention and euthanasia. Baseline IOP was measured by "minified" Goldmann applanation tonometry[25] using a Zeiss slit lamp (Carl Zeiss Meditec, Jena, Germany; average of three readings, 5 minutes apart, for all subsequent IOP measurements): SLE, tonometry, and perfusion measurement 5 weeks before surgical intervention; SLE weekly until no evidence of AC inflammation, usually within 4 to 5 weeks following measurements of outflow facility by perfusion method; SLE, tonometry, and corneal pachymetry 1 to 3 days prior to surgical intervention; and SLE, tonometry, and perfusion measurements 5 weeks prior to euthanasia.

Outflow Facility

Two methods were used in this study to measure outflow facility, perfusion (invasive) and pneumatonography (noninvasive).

Perfusion Technique. Outflow facility was determined by two-level constant pressure perfusion of the anterior chamber as previously described.[26] The ACs of both eyes were cannulated with one branched (placed superior-temporally) and one nonbranched (placed inferior-temporally) 26-gauge needle. One end of the branched needle was attached to an elevated reservoir containing Barany's solution[26] and the other to a pressure transducer. Tubing to the nonbranched needle was clamped. Baseline outflow facility was measured for 35 to 40 minutes. The tubing from the nonbranched needle was then attached to a variable speed infusion pump with the inflow line of the branched needle detached from the reservoir and open to air. Due to its invasive nature, perfusion measurements were performed at baseline and at the completion of recovery of all surgical interventions at the end of the experiment. A minimum 6-week recovery period following the measurements was required prior to the next surgical intervention.

Pneumatonography Technique. A pneumatonometer probe (Modular One tonometer; BioRad, Hercules, CA, USA) with the addition of a 10-g weight was placed and held perpendicular to the surface of the cornea. Prior to each measurement, the instruments were calibrated according to the manufacturer's instructions. Baseline IOP was calculated with the mean level of the recorded pulse wave. Two-minute tracings were obtained, and outflow facility was determined with the best linear fit from the tracings using pneumatonography tables and the standard formula for outflow facility calculation.[27] Mean values $\pm$ SD from four to five measurements performed over 1 week were obtained for the analysis. All test procedures were performed at baseline, at completion of recovery after each of the two surgical interventions, and at the end of the experiment.

PPV

As per standard surgical protocol, the animal was placed in supine position, and general anesthesia was induced. The animal's eyes were prepped and draped with care to completely separate the surgical field from the oxygen delivery with an adhesive surgical drape. Following placement of a lid speculum, a 30-gauge needle was used for entry into the AC, and the Oxylab O_2 optical oxygen sensor (optode; Oxford Optronix, Oxford, United Kingdom) was carefully introduced into the AC without leakage of aqueous humor (Fig. 1). Instrument calibration was performed prior to each experi-

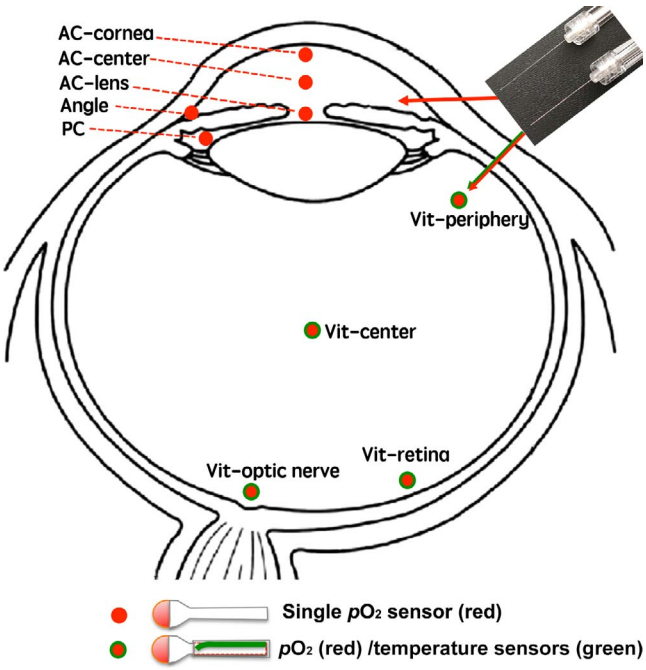

FIGURE 1. Diagram of oxygen measurement locations in monkey eye. Measurements were obtained at all locations at baseline and pre-euthanasia. AC, angle, and PC measurements were obtained at interim surgical interventions. *Red dot*, single fiberoptic element oxygen sensor used for the AC locations; *red/green dot,* dual fiberoptic element oxygen sensor plus temperature sensor used for vitreous chamber measurements; *arrows*, entry site for each sensor type.

ment by measuring established levels of pO_2 (0%, 2.5%, 5%, and 20%). Inaccurate or delayed measurements indicated probe failure. The tip of the flexible fiberoptic probe was positioned for three measurements by the surgeon (CJS; Fig. 1): (1) near the central corneal endothelium, (2) in the mid-AC, and (3) in the AC angle in both the surgical and the sham control eyes.

Following placement of the pars plana ports with the 23-gauge trocar device by the vitreoretinal surgeon (MN), and prior to initiating saline infusion, measurements were also obtained in the posterior chamber, in the pars plana region, midvitreous, and near the retina. Aqueous and vitreous humor specimens were obtained. PPV and sham PPV were then performed in opposite eyes of each monkey. Following the procedure, intraocular pO_2 measurements were repeated in the vitreous cavity. A subconjunctival injection of dexamethasone (0.2 mg) was performed. Postoperative examinations of biomicroscopy and tonometry were monitored for 3 to 5 months as indicated. Additional injections of dexamethasone were given postoperatively to manage inflammation, but no animal required more than three total injections or any beyond 6 weeks postoperatively.

PE/IOL

The preoperative measurements, assessments, and preparation for the surgical procedures were performed as described above for the PPV. Repeat pO_2 measurements were obtained as above excluding the vitreous cavity, and additional measurements were taken at the lens surface and in the posterior chamber (PC) in the surgery eye only. Aqueous humor samples were obtained. Lens extraction by phacoemulsification plus posterior chamber intraocular lens implantation (SN60 posterior chamber lens; Alcon, Inc., Fort Worth, TX, USA) and sham procedures were performed in the operated and control eyes

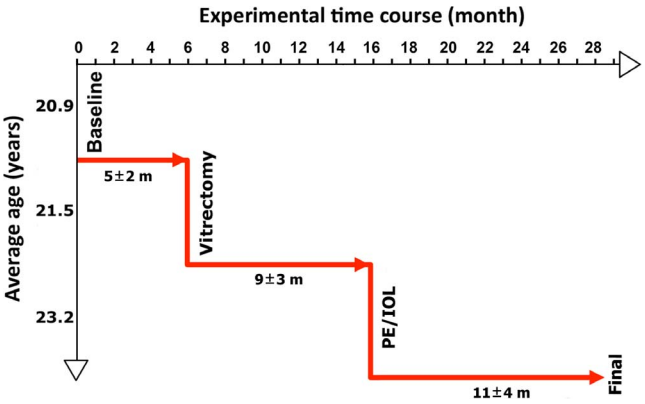

FIGURE 2. Experimental time course and monkey age progression during the study.

of each monkey by the anterior segment surgeon (GH), respectively, followed by a minimum 6-month observation period (Fig. 2).

Pre-Euthanasia Protocol

The preoperative measurements, assessments, and preparation for the final procedures were performed as described above. Prior to euthanasia, oxygen measurements were taken in the AC and at two locations in the vitreous chamber: at the vitreous periphery and center (Fig. 1). Aqueous and vitreous humor specimens were collected. Following anesthesia with IM ketamine (3 to 25 mg/kg), euthanasia was conducted with intravenous pentobarbital overdose (~50 mg/kg). Enucleation was performed, and the globes of the animals were sectioned. Optic nerve sections were fixed with 10% buffered formalin for H&E staining and optic nerve axon cell counts. Anterior segment sections were immediately dissected into two parts: half were embedded with optimal cutting temperature (OCT; Sakura Finetek, Torrance, CA, USA) medium and frozen on dry ice for TM laser micro-dissection, and half were fixed with 10% buffered formalin for histologic and immunochemistry analysis.

Aqueous and Vitreous Humor Analyses

All specimens were immediately transferred to receptacles in dry ice in the operating room and then transferred to a liquid nitrogen tank until analysis.

Ascorbic acid (AsA) concentrations in the aqueous humor and vitreous were measured as in our previous reports.[28] Briefly, a colorimetric assay was used to determine the AsA concentrations based on its reduction from Fe^{3+} to Fe^{2+} on reacting with 2,2′-dipyridyl. Assay modifications enabled the analysis of 10-μL samples, and a standard curve was used for all measurements. As a control for AsA specificity, two units of ascorbate oxidase (AO; A 0157; Sigma Chemical, St. Louis, MO, USA) was added to additional 10-μL samples, mixed well at room temperature, and then followed by AsA measurement in triplicate.

Total reactive antioxidant potential (TRAP) measurements were done. The TRAP assay is applied to determine the capacity of aqueous humor or vitreous to destroy free radicals in its solution as previously described.[29] Briefly, 2,2′-azobis(2-amidinopropane) (ABAP; Sigma Aldrich) and 40 μM luminol (3-aminophthalhydrazide; Sigma Aldrich) were added to a sample. ABAP combines with oxygen to produce alkyl peroxyl radicals at a constant rate. If antioxidant is absent, these radicals react with luminol to produce light, measured in a scintillation counter. However, if antioxidants are present, luminescence

will be quenched by peroxyl radical reactions. Because ABAP produces radicals at a constant rate, antioxidant activity is measured by the length of time that the test substance takes to quench luminescence. The assay is standardized using Trolox, a water-soluble vitamin E analog. Antioxidant potential is reported as "Trolox units," with one unit equal to amount of time that luminescence is quenched by a sample containing 1 μM Trolox. Replication of measurements were not performed due to limited sample volumes. Reproducible assays were completed in triplicate with human specimens ($n = 203$; Shui et al., unpublished data, 2014).

8-Hydroxy-2′-deoxyguanosine (8-OHdG) is a ubiquitous marker for oxidative damage. We used the OxiSelect Oxidative RNA Damage ELISA Kit (Cell Biolabs, Inc., San Diego, CA, USA) to detect 8-OHdG levels in the aqueous humor and vitreous samples. Fifty microliters of undiluted sample was used for the ELISA analysis following the product instruction manual. Duplicate measurements were not performed due to limited sample volumes in this study. ELISA techniques were previously validated in human samples in duplicate with confirmed reproducibility ($n = 3$; Shui et al., unpublished data, 2016).

Immunochemistry Staining

Formalin-fixed, paraffin-embedded monkey TM sections were used for immunochemistry staining. After deparaffinizing and antigen retrieval, two antibodies were applied to the same specimen. A mouse monoclonal antibody of 8-OHdG, (sc-393871; Santa Cruz Biotechnology, Dallas, TX, USA) was used at 1:500 dilution, and a rabbit polyclonal antibody of fibronectin (ab23751; Abcam, Cambridge, MA, USA) was used at 1:500 dilution at 4°C overnight, respectively. Alexa-Fluor 488 donkey anti-mouse IgG and Alexa-Fluor 555 donkey anti-rabbit IgG (1/1000; Abcam) were used as secondary antibodies to detect 8-OHdG and fibronectin separately. 4′,6-Diamidino-2-Phenylindole (DAPI) was used for nuclear staining. ImageJ (http://imagej.nih.gov/ij/; provided in the public domain by the National Institutes of Health, Bethesda, MD, USA) was used for fluorescence intensity analysis.

Histologic Staining for TM Cell and Optic Nerve Axon Counts

Formalin-fixed TM and optic nerve specimens were stained with hematoxylin and eosin. Light microscopic morphologic examinations and TM cell and axon cell counts were performed (ImageJ; Supplementary Fig. S1).

TM Laser Micro-Dissection and quantitative PCR Analysis

Fresh monkey anterior eye segments were embedded in OCT and immediately frozen on dry ice prior to storage at −80°C. Twelve-micrometer-thick frozen sections were transferred to glass polyethylene naphthalate foil slides (#11505189; Leica Microsystems, Wetzlar, Germany) as we previously described[30] and stained with Eosin Y. TM was dissected using a laser microdissection system (LMD 6000 and CTR 6500, Leica Microsystems) (Fig. 3). Some areas of uveal meshwork were included to obtain adequate RNA quantities. RNA extraction was performed using the RNeasy Micro Kit (Qiagen, Hilden, Germany) and amplification with Ovation Pico WTA System V2 (NuGEN Technologies, San Carlos, CA, USA). The quantitative PCR (qPCR) analysis was performed using LightCycler 480 Software according to manufacturer protocols. Quantified values for each gene of interest were normalized against the input determined by the housekeeping gene glyceraldehyde 3-phosphate dehydrogenase (GAPDH; Actb, NM_007393). We custom designed the primers for the monkey species to detect fibronectin, type IV collagen, and NF-κB (Supplementary Table S1). Each assay was performed in triplicate utilizing mean values for statistical analysis.

Statistical Analysis

Results are expressed as mean values ± SD. Statistical analyses were performed using GraphPad Prism (version 6.0; GraphPad, San Diego, CA, USA) and SPSS software Version 24.0 (SPSS, Chicago, IL, USA). A repeated-measures mixed model ANOVA was used to compare changes in outflow facility. Paired-samples *t*-tests were performed for comparisons of all other measurable parameters. Probability values less than 0.05 were considered statistically significant.

Results

Oxygen Measurements

Baseline pO_2 measurements demonstrated levels very similar to human patients in our previous studies[24,31] with noted steep oxygen gradients in the AC from 20.4 ± 1.8 mm Hg at the corneal endothelial surface decreasing to very low levels of 1.5 ± 0.8 mm Hg at the anterior lens surface (Fig. 4). Following vitrectomy surgery, pO_2 increased significantly in the PC from baseline of 6.2 ± 1.8 to 9.5 ± 1.5 mm Hg ($P < 0.05$) and increased additionally following PE/IOL implantation to 14.3 ± 2.0 mm Hg ($P < 0.05$). Following the second surgical intervention of PE/IOL implantation, statistically significant increases in pO_2 were also measured at the lens surface from baseline of 1.5 ± 0.8 to 11.9 ± 2.2 mm Hg ($P < 0.01$), in the AC angle from 11.3 ± 1.7 to 20.5 ± 2.4 mm Hg ($P < 0.01$), and in the center of the vitreous from baseline of 6.4 ± 1.5 to 12.7 ± 2.5 mm Hg ($P < 0.05$; Fig. 5). One monkey sustained a retinal detachment following the vitrectomy procedure, and only baseline measurements were included in the data analysis.

IOP

IOP measurements were compared between control and surgical eyes at the three time points and at each time point compared to baseline (Fig. 6). There was no difference in IOP at baseline between the two groups. There was a statistically significant increase in IOP in the surgical eyes from 19.1 ± 2.9 mm Hg at baseline to 22.6 ± 3.1 mm Hg after PPV/IOL placement ($P < 0.05$) and between the surgical (22.6 ± 3.1 mm Hg) and control eyes (17.4 ± 3.7 mm Hg) at the final time point ($P < 0.05$).

Outflow Facility Measurements

Measurements of outflow facility were performed by pneumatonography at baseline, after recovery from PPV, and after PE/IOL 6 weeks prior to euthanasia and by AC perfusion technique at baseline and after both surgical interventions 12 weeks before euthanasia. Neither technique revealed any significant differences in comparison between surgical and sham control and compared with baseline (Tables 1, 2). Repeated-measures mixed-model ANOVA did not identify $P < 0.05$ in any ratio comparisons.

Histologic Analysis

TM cell counts were performed from sections of the AC angle by a masked individual. No significant differences were

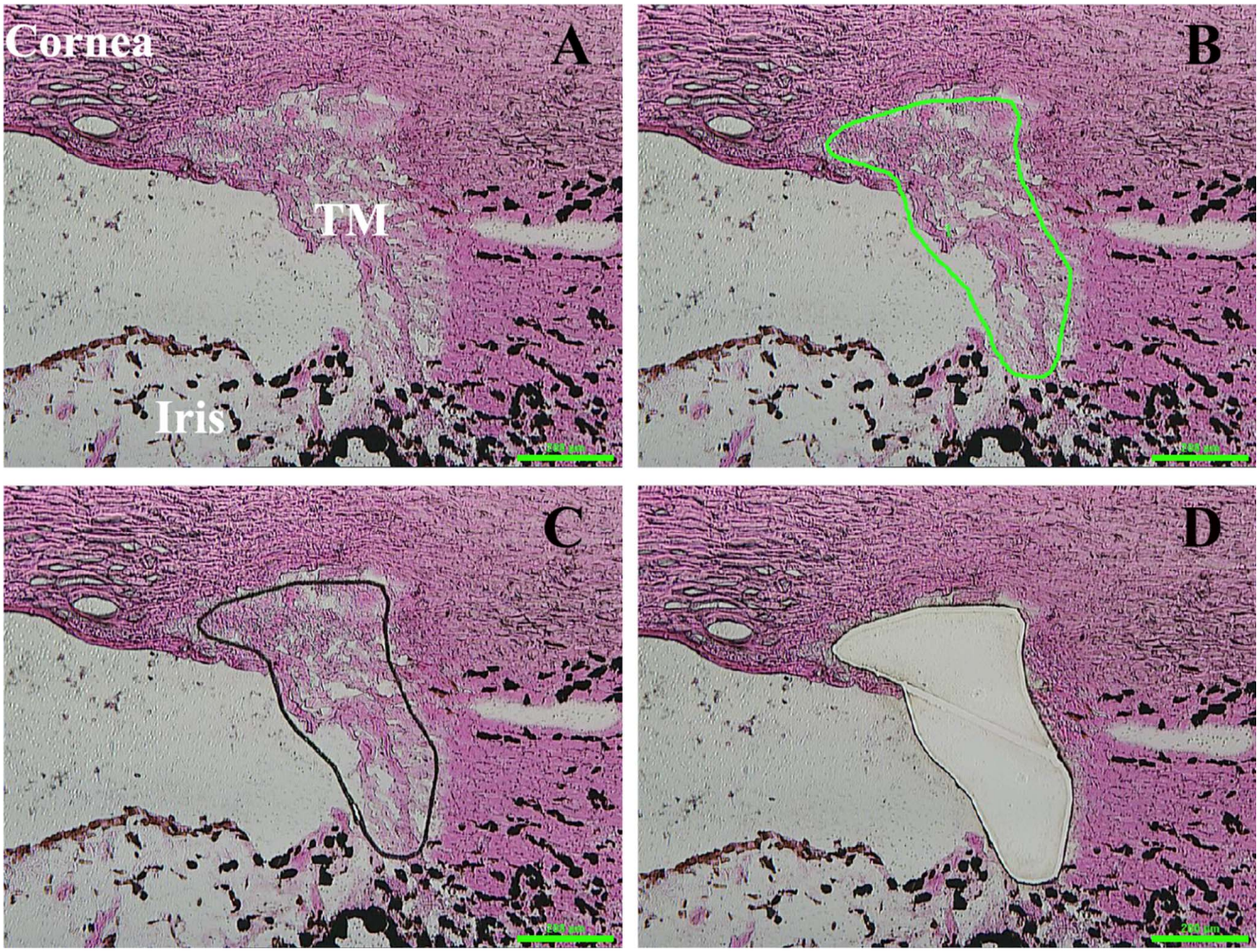

FIGURE 3. Laser dissection of fresh frozen TM tissues. (**A**) Baseline histologic image of AC angle region. (**B**) Laser pen delineation of TM (*green*). (**C**) Laser dissection of TM along outline. (**D**) TM tissue excised without contamination by adjacent tissues. *Green bar* at *lower right corner* of images: 200 μm.

measured between control and surgical eyes (Supplementary Fig. S1). No differences in optic nerve axon cell counts were noted between the surgical group and controls (data not shown).

TM Immunochemistry

AC angle specimens underwent immunochemistry staining for fibronectin and 8-OHdG (Fig. 7). Although there appeared to be an increase in fibronectin deposition in the surgical group, further quantification by fluorescence density measurements did not confirm this finding. Only 8-OHdG revealed a statistically significant increase of fluorescence density following the surgical interventions (16.6 ± 4.5) compared with controls (8.8 ± 3.4, $P = 0.012$). The diffuse distribution of 8-OHdG throughout the extracellular matrix and the fibronectin appeared to be more granular with deposition in the TM cell cytoplasm. No differences were identified in immunochemistry staining for type IV collagen and NF-κB in specimens from control and surgical eyes (data not shown).

qPCR Analysis of TM

TM specimens underwent precise laser micro-dissection to isolate the TM for qPCR analysis, using specific macaque primers (Supplementary Table S1). Paired *t*-test analysis did not show significant differences in fibronectin or NF-κB expression in the TM of the control versus surgical eyes (Supplementary Fig. S2).

Aqueous and Vitreous Humor Analysis

AsA levels significantly decreased in surgical eyes compared with baseline in both aqueous (1.55 ± 0.12 to 1.11 ± 0.21 mM, $P = 0.002$) (Fig. 8) and vitreous humor specimens (2.03 ± 0.35 to 1.29 ± 0.2 mM, $P = 0.02$). TRAP was also decreased in the aqueous (440 ± 79 to 369 ± 43 Trolox units, $P = 0.01$) and vitreous (568 ± 96 to 432 ± 62 Trolox units, $P < 0.03$) in the surgical group (Fig. 8). There were no differences in either AsA or TRAP in baseline measurements of the control group compared with the surgical group. 8-OHdG levels in aqueous humor were increased after PPV compared with control (0.60 ± 0.25 versus 0.36 ± 0.29 ng/mL, $P = 0.03$) and further increased compared with control after PE/IOL (0.77 ± 0.36 versus 0.51 ± 0.3 ng/mL, $P = 0.02$) (Fig. 9). There were no significant differences in 8-OHdG levels measured in vitreous humor specimens collected at the conclusion of the study comparing the PPV/IOL group and controls (Fig. 9).

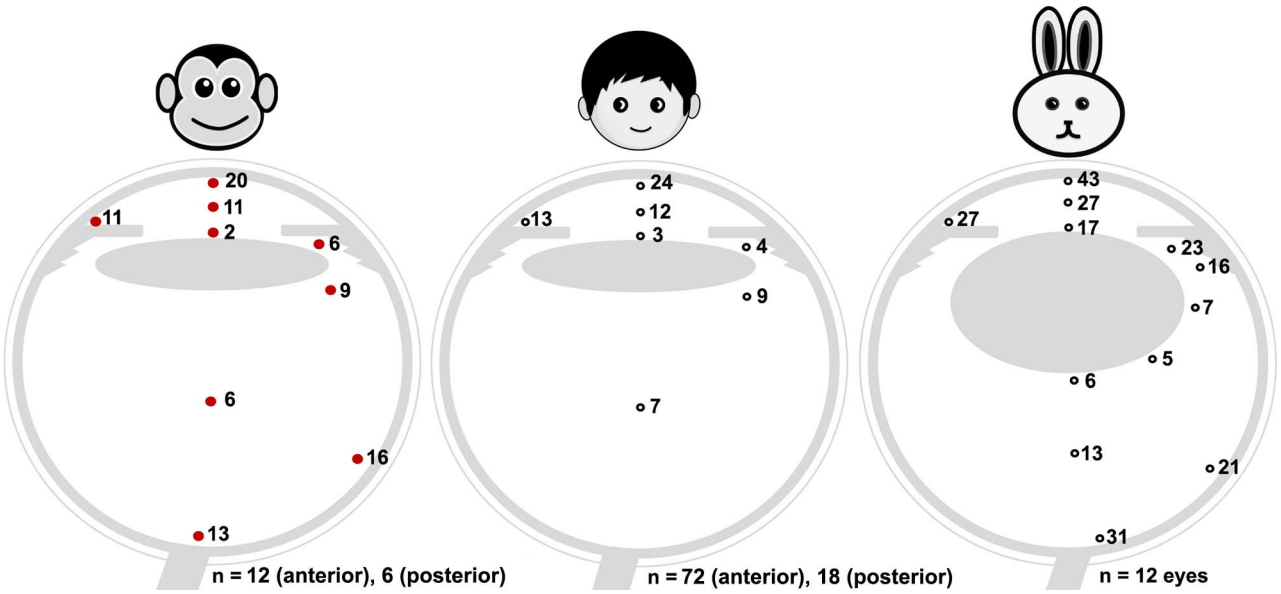

Figure 4. Comparison of mean intraoperative baseline oxygen distribution in monkey, human, and rabbit eyes at noted locations (mm Hg). Both eyes of six monkeys underwent baseline measurements in the AC, but only the surgical eye was included for pO_2 measurements in the vitreous and adjacent to the lens. The human study was comprised of reference group undergoing cataract extraction (anterior segment measurements)[24] and patients undergoing PPV (posterior segment measurements).[33] Oxygen distribution in rabbit eyes[32] is also displayed for comparison.

Discussion

Our precise techniques of intraocular pO_2 measurements have confirmed stable oxygen gradients in a variety of species.[24,31–33] This current study is the first to demonstrate that PPV leads to a significant increase in pO_2 in the AC angle and PC of this nonhuman primate species. Unlike human patients, however, we did not observe development of nuclear sclerotic cataract following PPV, which may relate to the limited mean time interval for observation and assessment (9 ± 3 months), as well as other yet unknown factors. This phenomenon has not been described in any other species to date. As in our human patients, the baseline environment surrounding the lens is quite hypoxic, increasing in the PC but not at the anterior surface of the lens after vitrectomy surgery. Our human studies did not confirm correlations of increased pO_2 in any intraocular location following any surgical intervention with glaucoma diagnosis

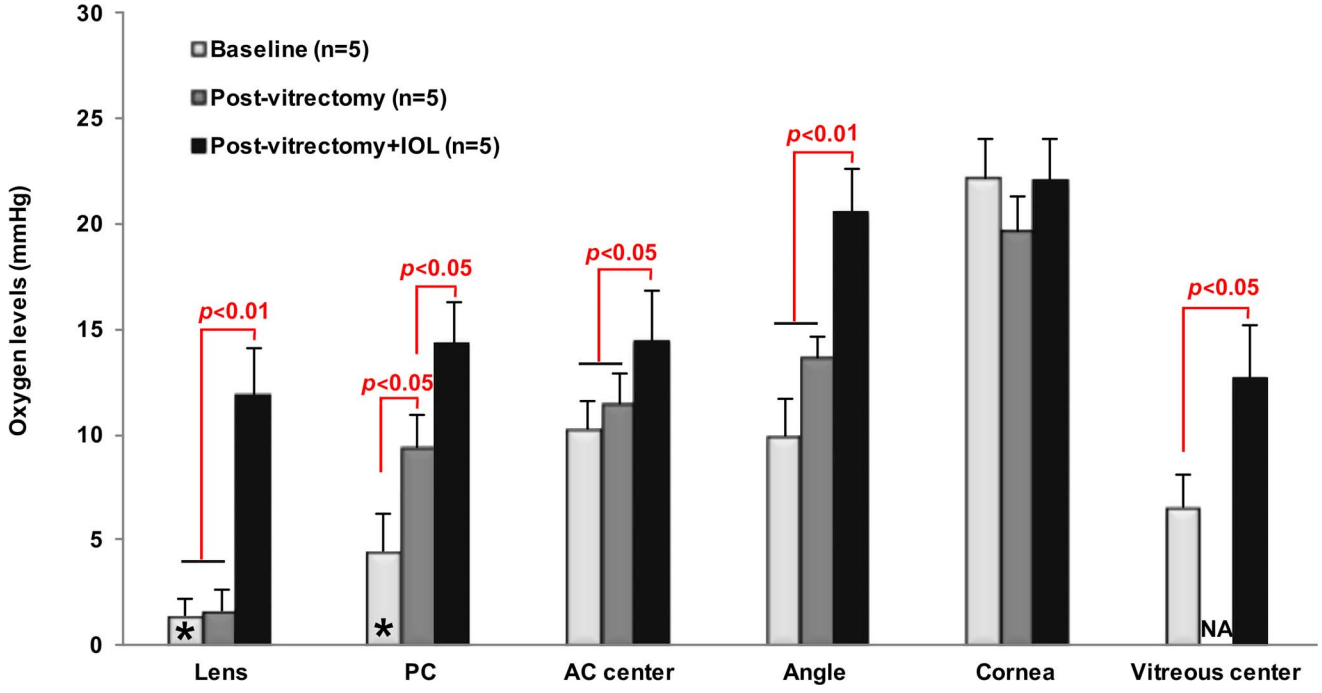

Figure 5. Intraocular oxygen measurements at baseline and after each surgical intervention at specific intraocular locations. All measurements are from surgical eye except at the lens and PC (baseline*), which were obtained from the control eye before euthanasia. Data values: mean ± SD. Paired-samples *t*-test was used for statistical analysis. NA, no measurement performed.

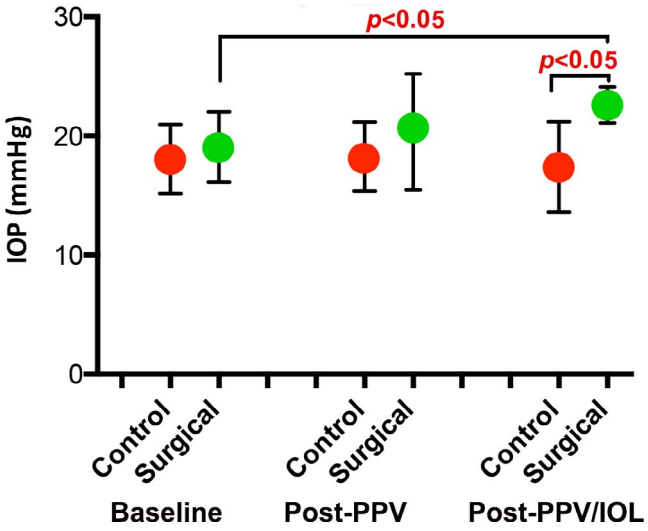

FIGURE 6. IOP at baseline and after each surgical intervention. Data values: mean ± SD, $n = 5$.

(Siegfried et al., unpublished data, 2016). We hypothesized that prolonged exposure to increased pO_2 after PPV/IOL may be a risk factor for the development of open angle glaucoma. We previously reported inverse correlations of pO_2 in the AC angle with central corneal thickness,[34] as well as increased pO_2 in all measured locations in African-American subjects compared with Caucasians.[35] Central corneal thickness[36–38] and African racial descent[39–43] have both been identified as important independent risk factors for both development and progression of open angle glaucoma.

"Oxidative stress" is defined as an increase of intracellular concentrations of reactive oxygen species (ROS), including hydrogen peroxide, singlet oxygen, superoxide anion, and hydroxyl and peroxyl radicals. Oxidative stress, and the imbalance of ROS and antioxidants, may lead to oxidative damage of cellular components including DNA, enzymatic and structural proteins, and membrane lipids. Oxidative damage has been identified as playing a role in several ocular diseases including Fuchs' corneal dystrophy,[44] age-related cataract,[45] macular degeneration,[46] and diabetic retinopathy.[47] The contribution of oxidative damage to the pathogenesis of glaucomatous optic neuropathy has been described in a multitude of studies,[48–51] but the source of these free radicals and/or alterations of the oxidant–antioxidant balance have not been confirmed in the eye. Sacca et al. demonstrated that oxidative stress initially damages TM cells and subsequently alters nitric oxide and endothelin homeostasis, resulting in the final end point of glaucomatous loss of retinal ganglion cells.[52] TM mitochondrial damage also plays a key role[53] as these organelles are an important endogenous source of ROS.[54]

Many studies provide evidence of oxidative damage and reduced resistance to oxidative stress in the outflow pathway and in retinal ganglion cell degeneration.[51,55] Increased DNA oxidative damage has been documented in TM cells of glaucoma patients compared with controls,[56] correlating with IOP level and visual field loss.[57] Increased levels of 8-hydroxy-2′-deoxyguanosine, a recognized biomarker of oxidative DNA damage, have been observed in the serum and aqueous humor of glaucoma patients,[58] in addition to TM of patients with open angle glaucoma as noted above. In our present study, the limited observation time after surgical interventions may have reduced our ability to detect significant changes in TM function as measured by outflow facility, although statistically significant increases in IOP were documented in surgical eyes versus control. This IOP increase is consistent with several human postvitrectomy studies with 12 to 57 months of follow-up,[14–17,20] including an ongoing prospective study.[23] We identified increased levels of 8-OHdG in aqueous humor following PPV/IOL compared with control monkey eyes. This finding was not confirmed in vitreous specimens, suggesting this biomarker of oxidant damage specifically identified indirect evidence of oxidative damage in the structures of the anterior segment bathed by aqueous humor. 8-OHdG has been identified in various body fluids and tissues including cerebrospinal fluid, serum, and urine.[59,60] The modified DNA is excised and exported into extracellular fluids. Levels of 8-OHdG in cerebrospinal fluid may reflect severity and duration of neurodegenerative disease.[61]

Ocular exposure to visible and ultraviolet light irradiation is greater than any other organ except skin; therefore, protective antioxidant mechanisms are required to prevent cellular oxidative damage caused by ROS. As ROS are defined by their high reactivity and transient nature, these elements cannot be measured in a direct assay.[62] Research involving these molecules requires indirect analysis via antioxidant assays. Extremely high levels of AsA have been measured in aqueous and vitreous humor,[28,63] as well as corneal epithelium[64] and lens,[65] compared with plasma in diurnal animals. Shui et al.[28] showed in ex vivo experiments that molecular oxygen metabolism in vitreous gel is AsA dependent and that AsA is the principal regulator of intraocular oxygen. In vivo pO_2 measurements in human subjects performed immediately (75.6 ± 4.1 mm Hg) and months to years after vitrectomy surgery (13.3 ± 0.8 mm Hg) were significantly higher compared with baseline prior to vitrectomy surgery (7.1 ± 0.5 mm Hg; $P < 0.0001$ and $P < 0.003$, respectively).[33] Other water-soluble molecules and enzymes such as glutathione, superoxide dismutase, catalase, and glutathione peroxidase also play a role in aqueous humor antioxidant protection, but we identified AsA as the most significant component (approximately 75%) of human aqueous humor TRAP, a "global" measure of antioxidant status (Siegfried et al., unpublished data, 2016). Our current findings of significantly decreased levels of AsA and TRAP in aqueous and vitreous humor specimens after PPV/IOL suggest antioxidant depletion in the presence of increased oxidative stress. Increased pO_2 in the anterior and posterior segments after vitrectomy and lens extraction may be a source of these ROS, which cannot be accurately quantified as noted above. In contrast, PE/IOL without vitrectomy does not result in statistically significant

TABLE 1. Monkey Outflow Facility Measured by Pneumatonography Technique

	μL/mim/mm Hg							
	Control	Surgical	Surg/Cont	Surg/BL	Cont/BL	Surg (% of BL)	Cont (% of BL)	(Surg/BL)/(Cont/BL)
Baseline	0.534 ± 0.20	0.516 ± 0.18	1.028 ± 0.13	-	-	-	-	-
Post-PPV	0.444 ± 0.15	0.403 ± 0.11	0.929 ± 0.08	0.878 ± 0.16	0.907 ± 0.14	87.8 ± 16.13	90.7 ± 13.96	0.954 ± 0.13
Post-PPV/IOL	0.399 ± 0.18	0.315 ± 0.17	0.783 ± 0.10	0.704 ± 0.20	0.888 ± 0.28	70.4 ± 19.52	88.8 ± 27.63	0.835 ± 0.17

$n = 5$ at all time points. Data values: mean ± SD. Ratios are unitless. BL, baseline; Cont, sham control eye; Surg, surgical eye.

Table 2. Monkey Outflow Facility Measured by AC Perfusion Technique

	μL/mim/mm Hg							
	Control	Surgical	Surg/Cont	Cont/BL	Surg/BL	Cont (% of BL)	Surg (% of BL)	(Surg/BL)/ (Cont/BL)
Baseline	0.307 ± 0.04	0.379 ± 0.07	1.245 ± 0.10	–	–	–	–	–
Post-PPV/IOL	0.268 ± 0.03	0.352 ± 0.04	1.330 ± 0.12	0.888 ± 0.07	0.940 ± 0.05	88.8 ± 6.86	93.984 ± 4.53	1.083 ± 0.09

$n = 5$ at all time points. Data values: mean ± SD. Ratios are unitless.

increased pO_2 in the AC angle.[24] In these cases, postoperative IOP is reduced and has been theorized to be due to anatomic/biometric parameter changes,[66] posterior movement of the lens diaphragm dilating Schlemm's canal, and increasing aqueous outflow,[67] as well as possible induction of inflammatory cytokines by ultrasonic phacoemulsification energy, which may stimulate metalloproteinase production and remodeling of the trabecular meshwork.[68]

A recently published systematic review and meta-analysis of oxidant–antioxidant stress markers in serum and aqueous humor[69] also demonstrated a decreased total antioxidant status in both fluids in glaucoma patients compared with controls

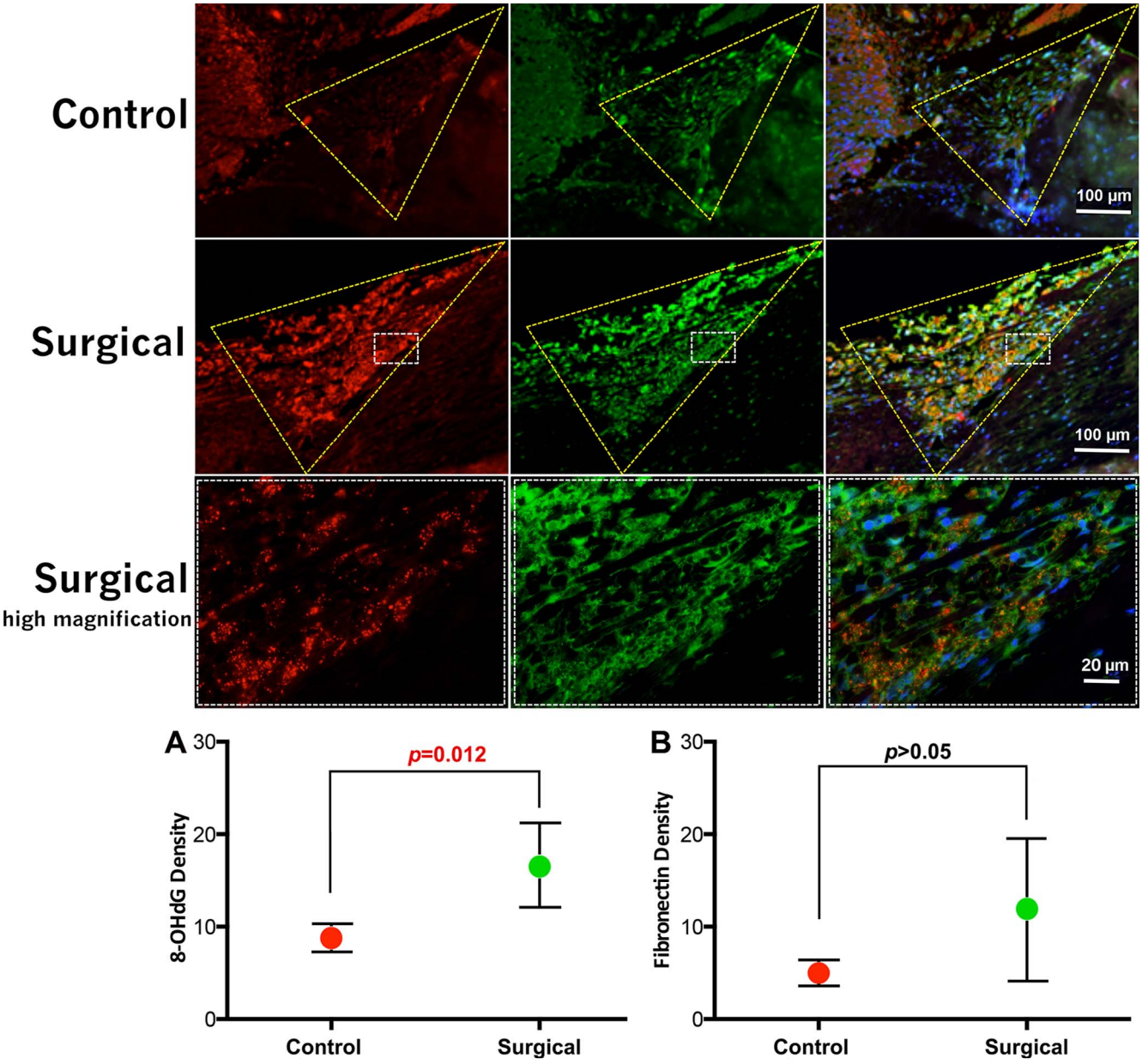

Figure 7. Immunohistochemical staining of trabecular meshwork from monkeys after surgical interventions. Fluorescence density measurements of fibronectin (*red*) and 8-OHdG (*green*) and merged with DAPI (nuclear staining). High-magnification images show differing distributions of fibronectin (*red*), 8-OHdG (*green*) in the trabecular meshwork, and merged image with DAPI. Data values = mean ± SD, $n = 5$. Scale bars denote 20 and 100 μm. (**A**) Quantitative fluorescence densities for 8-OHdG and (**B**) fibronectin.

Investigative Ophthalmology & Visual Science

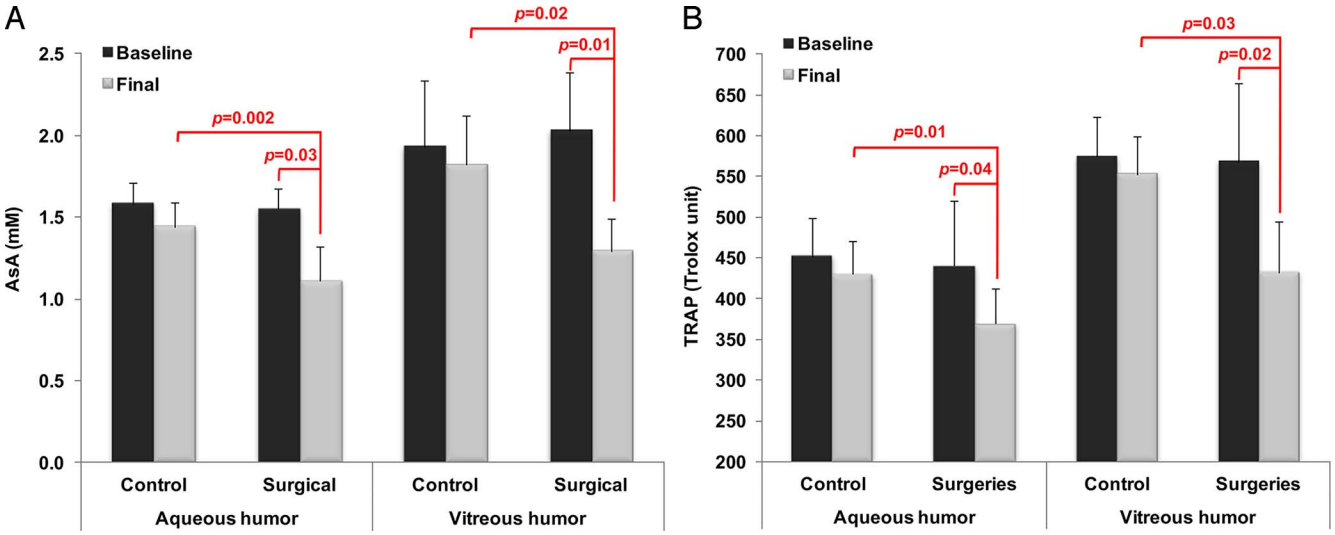

FIGURE 8. (A) AsA levels in aqueous and vitreous humor. (B) TRAP assay of aqueous and vitreous at baseline and after surgical interventions. $n = 5$. Paired-samples t-test used for statistical analysis.

(patients undergoing cataract surgery). The antioxidant decrease was greatest in serum specimens and most closely correlated with the biomarker malonydialdehyde. TRAP is decreased in glaucoma patients and animal models,[29,70,71] but AsA has shown both increased[63] and decreased levels in primary open and pseudoexfoliative glaucoma patients compared with a control cataract group.[29] In our study of glaucoma patients, we did not identify changes in AsA levels but did find a compensatory increase in non–AsA-dependent TRAP levels (Siegfried et al., unpublished data, 2016). This complex balance of oxidant–antioxidant status within the eye requires further study of correlations and compensatory mechanisms.

In our TM analysis, we did not identify loss of cellularity or other morphologic changes characteristic of primary open angle glaucoma. Oxidative stress may affect TM cells by activation of the NF-κB pathway,[72,73] as well as alter the extracellular matrix composition including deposition of fibronectin.[74] qPCR analyses for NF-κB and fibronectin, potential markers of glaucomatous pathology, did not reach statistical significance. However, a biomarker of oxidative damage, 8-OHdG, was notably increased in TM tissue, perhaps an early finding prior to functional damage associated with decreased outflow facility. TM tissue is more sensitive to oxidative damage than other ocular tissues, as assessed by hydrogen peroxide exposure.[75] Oxidative damage to DNA is also greater specifically in the TM of glaucoma patients compared with controls[56] and correlates with visual field loss and IOP.[57]

Our selection of this older primate in middle age (equivalent to 50 to 55 human years) has limitations due to the restricted subject number and short period of postsurgical follow-up for a disease of oxidative damage that may take several years to alter TM structure and function. These factors may explain the lack of significant changes in our measured parameters. The qPCR analysis may not have been directed at appropriate genes for study, and perhaps future studies including broad analysis with differential gene expression will be more productive.

Oxidative damage to the TM, an important factor in the development of open angle glaucoma, is not well understood in terms of initiating factors other than as an "age-related" phenomenon. We hypothesize that specific factors, such as increased oxygen levels, may affect the local environment of the AC angle. This may alter this region's oxidant–antioxidant

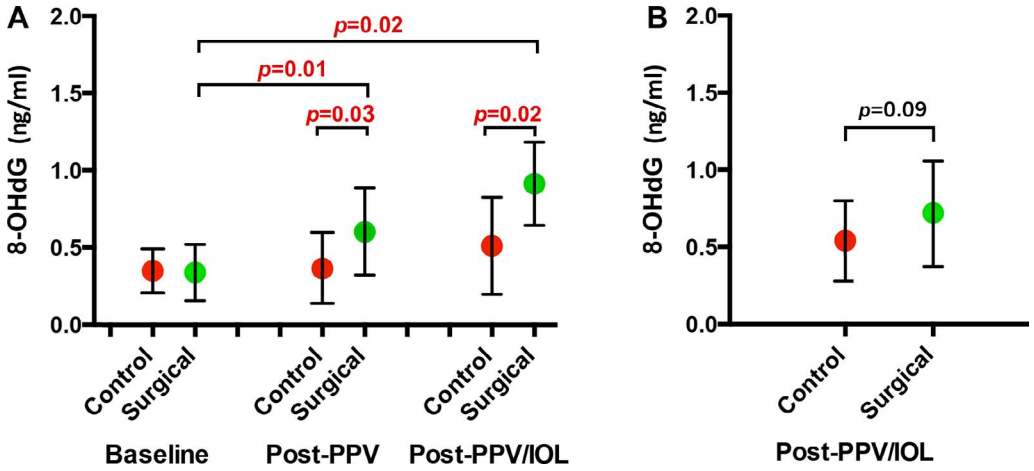

FIGURE 9. (A) 8-OHdG levels in aqueous humor at surgical interventions. (B) Vitreous humor obtained before euthanasia (post-PPV/IOL). Data values = mean ± SD, $n = 5$. Paired-samples t-test used for data analysis.

status, resulting in increased exposure to ROS. Our current analysis of aqueous humor specimens in this animal model suggests that antioxidant potential, reflected in decreased AsA and TRAP levels, is depleted in the presence of increased free radicals. Increased IOP and biomarker evidence of oxidative damage in both the TM and aqueous humor may provide insight into how oxygen homeostasis alters one's risk of open angle glaucoma after vitrectomy and potentially lead to future targeted therapies for this blinding condition.

Acknowledgments

The authors thank Brad Wilson, MA, for assistance with statistical analyses; Fang Bai, MD, for assistance with the TRAP assay; Ying Liu, BS, for assistance with laser microdissection and PCR analysis; Julie Kiland and Jared McDonald for technical assistance with intraoperative and postoperative care of the monkeys; Galen Heyne and Alex Katz for assistance with outflow facility measurements; and David Beebe, PhD, for inspiration and guidance in the planning phase of this project.

Supported by National Eye Institute Grant NEI-EY021515 (CJS), Core Grant NEI P30 EY02687 to Washington University (WU), Core Grant NEI P30 EY016665 to University of Wisconsin-Madison (UW), Glaucoma Research Foundation Shaffer Grant (CJS), McPherson Eye Research Institute's Retina Research Foundation Kathryn & Latimer Murfee Chair (TMN), Alcon Research, Ltd., and unrestricted grants from Research to Prevent Blindness, Inc. to both WU and UW.

Disclosure: **C.J. Siegfried**, Alcon Research, Ltd. (F); **Y.-B. Shui**, None; **B. Tian**, None; **T.M. Nork**, None; **G.A. Heatley**, None; **P.L. Kaufman**, None

References

1. Machemer R, Buettner H, Norton EW, Parel JM. Vitrectomy: a pars plana approach. *Trans Am Acad Ophthalmol Otolaryngol*. 1971;75:813–820.
2. Schulz-Key S, Carlsson JO, Crafoord S. Longterm follow-up of pars plana vitrectomy for vitreous floaters: complications, outcomes and patient satisfaction. *Acta Ophthalmol*. 2011; 89:159–165.
3. Stein JD, Zacks DN, Grossman D, Grabe H, Johnson MW, Sloan FA. Adverse events after pars plana vitrectomy among medicare beneficiaries. *Arch Ophthalmol*. 2009;127:1656–1663.
4. Wubben TJ, Talwar N, Blachley TS, et al. Rates of vitrectomy among enrollees in a United States Managed Care Network, 2001-2012. *Ophthalmology*. 2016;123:590–598.
5. Novak MA, Rice TA, Michels RG, Auer C. The crystalline lens after vitrectomy for diabetic retinopathy. *Ophthalmology*. 1984;91:1480–1484.
6. de Bustros S, Thompson JT, Michels RG, Enger C, Rice TA, Glaser BM. Nuclear sclerosis after vitrectomy for idiopathic epiretinal membranes. *Am J Ophthalmol*. 1988;105:160–164.
7. Cherfan GM, Michels RG, de Bustros S, Enger C, Glaser BM. Nuclear sclerotic cataract after vitrectomy for idiopathic epiretinal membranes causing macular pucker. *Am J Ophthalmol*. 1991;111:434–438.
8. Melberg NS, Thomas MA. Nuclear sclerotic cataract after vitrectomy in patients younger than 50 years of age. *Ophthalmology*. 1995;102:1466–1471.
9. Panozzo G, Parolini B. Cataracts associated with posterior segment surgery. *Ophthalmol Clin North Am*. 2004;17:557–568.
10. Feng H, Adelman RA. Cataract formation following vitreoretinal procedures. *Clin Ophthalmol*. 2014;8:1957–1965.
11. Eaton JW. Is the lens canned? *Free Radic Biol Med*. 1991;11: 207–213.
12. Almony A, Holekamp NM, Bai F, Shui YB, Beebe D. Small-gauge vitrectomy does not protect against nuclear sclerotic cataract. *Retina*. 2012;32:499–505.
13. Harocopos GJ, Shui YB, McKinnon M, Holekamp NM, Gordon MO, Beebe DC. Importance of vitreous liquefaction in age-related cataract. *Invest Ophthalmol Vis Sci*. 2004;45: 77–85.
14. Koreen L, Yoshida N, Escariao P, et al. Incidence of, risk factors for, and combined mechanism of late-onset open-angle glaucoma after vitrectomy. *Retina*. 2012;32:160–167.
15. Luk FO, Kwok AK, Lai TY, Lam DS. Presence of crystalline lens as a protective factor for the late development of open angle glaucoma after vitrectomy. *Retina*. 2009;29:218–224.
16. Wu L, Berrocal MH, Rodriguez FJ, et al. Intraocular pressure elevation after uncomplicated pars plana vitrectomy: results of the Pan American Collaborative Retina Study Group. *Retina*. 2014;34:1985–1989.
17. Toyokawa N, Kimura H, Matsumura M, Kuroda S. Incidence of late-onset ocular hypertension following uncomplicated pars plana vitrectomy in pseudophakic eyes. *Am J Ophthalmol*. 2015;159:727–732.
18. Yamamoto K, Iwase T, Terasaki H. Long-term changes in intraocular pressure after vitrectomy for rhegmatogenous retinal detachment, epi-retinal membrane, or macular hole. *PLoS One*. 2016;11:e0167303.
19. Chang S. LXII Edward Jackson lecture: open angle glaucoma after vitrectomy. *Am J Ophthalmol*. 2006;141:1033–1043.
20. Mi CW, Thompson JT. Long-term follow-up of intraocular pressure after vitrectomy in eyes without preexisting glaucoma. *Retina*. 2015;35:2543–2551.
21. Yu AL, Brummeisl W, Schaumberger M, Kampik A, Welge-Lussen U. Vitrectomy does not increase the risk of open-angle glaucoma or ocular hypertension: a 5-year follow-up. *Graefes Arch Clin Exp Ophthalmol*. 2010;248:1407–1414.
22. Lalezary M, Kim SJ, Jiramongkolchai K, Recchia FM, Agarwal A, Sternberg P Jr. Long-term trends in intraocular pressure after pars plana vitrectomy. *Retina*. 2011;31:679–685.
23. Lalezary M, Shah RJ, Reddy RK, et al. Prospective Retinal and Optic Nerve Vitrectomy Evaluation (PROVE) study: twelve-month findings. *Ophthalmology*. 2014;121:1983–1989.
24. Siegfried CJ, Shui YB, Holekamp NM, Bai F, Beebe DC. Oxygen distribution in the human eye: relevance to the etiology of open-angle glaucoma after vitrectomy. *Invest Ophthalmol Vis Sci*. 2010;51:5731–5738.
25. Kaufman PL, Davis GE. "Minified" Goldmann applanating prism for tonometry in monkeys and humans. *Arch Ophthalmol*. 1980;98:542–546.
26. Barany EH. Simultaneous measurement of changing intraocular pressure and outflow facility in the vervet monkey by constant pressure infusion. *Invest Ophthalmol Vis Sci*. 1964; 3:135–143.
27. Langham ME, Leydhecker W, Krieglstein G, Waller W. Pneumatonographic studies on normal and glaucomatus eyes. *Adv Ophthalmol*. 1976;32:108–133.
28. Shui YB, Holekamp NM, Kramer BC, et al. The gel state of the vitreous and ascorbate-dependent oxygen consumption: relationship to the etiology of nuclear cataracts. *Arch Ophthalmol*. 2009;127:475–482.
29. Ferreira SM, Lerner SF, Brunzini R, Evelson PA, Llesuy SF. Oxidative stress markers in aqueous humor of glaucoma patients. *Am J Ophthalmol*. 2004;137:62–69.
30. Ma N, Siegfried C, Kubota M, et al. Expression profiling of ascorbic acid-related transporters in human and mouse eyes. *Invest Ophthalmol Vis Sci*. 2016;57:3440–3450.
31. Siegfried CJ, Shui YB, Holekamp NM, Bai F, Beebe DC. Oxygen distribution in the human eye: relevance to the etiology of

open angle glaucoma after vitrectomy. *Invest Ophthalmol Vis Sci*. 2010;51:5731–5738.

32. Shui YB, Fu JJ, Garcia C, et al. Oxygen distribution in the rabbit eye and oxygen consumption by the lens. *Invest Ophthalmol Vis Sci*. 2006;47:1571–1580.
33. Holekamp NM, Shui YB, Beebe DC. Vitrectomy surgery increases oxygen exposure to the lens: a possible mechanism for nuclear cataract formation. *Am J Ophthalmol*. 2005;139: 302–310.
34. Siegfried CJ, Shui YB, Bai F, Beebe DC. Central corneal thickness correlates with oxygen levels in the human anterior chamber angle. *Am J Ophthalmol*. 2015;159:457–462.
35. Siegfried CJ, Shui YB, Holekamp NM, Bai F, Beebe DC. Racial differences in ocular oxidative metabolism: implications for ocular disease. *Arch Ophthalmol*. 2011;129:849–854.
36. Gordon MO, Beiser JA, Brandt JD, et al. The Ocular Hypertension Treatment Study: baseline factors that predict the onset of primary open-angle glaucoma. *Arch Ophthalmol*. 2002;120:714–720; discussion 829–730.
37. Gordon MO, Torri V, Miglior S, et al. Validated prediction model for the development of primary open-angle glaucoma in individuals with ocular hypertension. *Ophthalmology*. 2007;114:10–19.
38. Leske MC, Heijl A, Hyman L, Bengtsson B, Dong L, Yang Z. Predictors of long-term progression in the early manifest glaucoma trial. *Ophthalmology*. 2007;114:1965–1972.
39. Tielsch JM, Sommer A, Katz J, Royall RM, Quigley HA, Javitt J. Racial variations in the prevalence of primary open-angle glaucoma. The Baltimore Eye Survey. *JAMA*. 1991;266:369–374.
40. Javitt JC, McBean AM, Nicholson GA, Babish JD, Warren JL, Krakauer H. Undertreatment of glaucoma among black Americans. *N Engl J Med*. 1991;325:1418–1422.
41. Munoz B, West SK, Rubin GS, et al. Causes of blindness and visual impairment in a population of older Americans: the Salisbury Eye Evaluation Study. *Arch Ophthalmol*. 2000;118: 819–825.
42. Wilson R, Richardson TM, Hertzmark E, Grant WM. Race as a risk factor for progressive glaucomatous damage. *Ann Ophthalmol*. 1985;17:653–659.
43. Leske MC, Connell AM, Schachat AP, Hyman L. The Barbados Eye Study. Prevalence of open angle glaucoma. *Arch Ophthalmol*. 1994;112:821–829.
44. Buddi R, Lin B, Atilano SR, Zorapapel NC, Kenney MC, Brown DJ. Evidence of oxidative stress in human corneal diseases. *J Histochem Cytochem*. 2002;50:341–351.
45. Truscott RJ. Age-related nuclear cataract-oxidation is the key. *Exp Eye Res*. 2005;80:709–725.
46. Zarbin MA. Current concepts in the pathogenesis of age-related macular degeneration. *Arch Ophthalmol*. 2004;122: 598–614.
47. Tewari S, Santos JM, Kowluru RA. Damaged mitochondrial DNA replication system and the development of diabetic retinopathy. *Antioxid Redox Signal*. 2012;17:492–504.
48. Alvarado J, Murphy C, Polansky J, Juster R. Age-related changes in trabecular meshwork cellularity. *Invest Ophthalmol Vis Sci*. 1981;21:714–727.
49. Sacca SC, Izzotti A, Rossi P, Traverso C. Glaucomatous outflow pathway and oxidative stress. *Exp Eye Res*. 2007; 84:389–399.
50. Zhou L, Li Y, Yue BY. Oxidative stress affects cytoskeletal structure and cell-matrix interactions in cells from an ocular tissue: the trabecular meshwork. *J Cell Physiol*. 1999;180: 182–189.
51. Green K. Free radicals and aging of anterior segment tissues of the eye: a hypothesis. *Ophthalmic Res*. 1995;27(Suppl 1): 143–149.
52. Sacca SC, Izzotti A. Oxidative stress and glaucoma: injury in the anterior segment of the eye. *Prog Brain Res*. 2008;173: 385–407.
53. Izzotti A, Sacca SC, Longobardi M, Cartiglia C. Mitochondrial damage in the trabecular meshwork of patients with glaucoma. *Arch Ophthalmol*. 2010;128:724–730.
54. Indo HP, Davidson M, Yen HC, et al. Evidence of ROS generation by mitochondria in cells with impaired electron transport chain and mitochondrial DNA damage. *Mitochondrion*. 2007;7:106–118.
55. Chen JZ, Kadlubar FF. A new clue to glaucoma pathogenesis. *Am J Med*. 2003;114:697–698.
56. Izzotti A, Sacca SC, Cartiglia C, De Flora S. Oxidative deoxyribonucleic acid damage in the eyes of glaucoma patients. *Am J Med*. 2003;114:638–646.
57. Sacca SC, Pascotto A, Camicione P, Capris P, Izzotti A. Oxidative DNA damage in the human trabecular meshwork: clinical correlation in patients with primary open-angle glaucoma. *Arch Ophthalmol*. 2005;123:458–463.
58. Sorkhabi R, Ghorbanihaghjo A, Javadzadeh A, Rashtchizadeh N, Moharrery M. Oxidative DNA damage and total antioxidant status in glaucoma patients. *Mol Vis*. 2011;17:41–46.
59. Loft S, Poulsen HE. Markers of oxidative damage to DNA: antioxidants and molecular damage. *Methods Enzymol*. 1999; 300:166–184.
60. Shigenaga MK, Gimeno CJ, Ames BN. Urinary 8-hydroxy-2′-deoxyguanosine as a biological marker of in vivo oxidative DNA damage. *Proc Natl Acad Sci U S A*. 1989;86:9697–9701.
61. Gmitterova K, Heinemann U, Gawinecka J, et al. 8-OHdG in cerebrospinal fluid as a marker of oxidative stress in various neurodegenerative diseases. *Neurodegener Dis*. 2009;6:263–269.
62. Pryor WA, Godber SS. Noninvasive measures of oxidative stress status in humans. *Free Radic Biol Med*. 1991;10:177–184.
63. Lee P, Lam KW, Lai M. Aqueous humor ascorbate concentration and open-angle glaucoma. *Arch Ophthalmol*. 1977;95: 308–310.
64. Ringvold A. In vitro evidence for UV-protection of the eye by the corneal epithelium mediated by the cytoplasmic protein, RNA, and ascorbate. *Acta Ophthalmol Scand*. 1997;75:496–498.
65. Reddy VN, Giblin FJ, Lin LR, Chakrapani B. The effect of aqueous humor ascorbate on ultraviolet-B-induced DNA damage in lens epithelium. *Invest Ophthalmol Vis Sci*. 1998;39:344–350.
66. Poley BJ, Lindstrom RL, Samuelson TW, Schulze R Jr. Intraocular pressure reduction after phacoemulsification with intraocular lens implantation in glaucomatous and non-glaucomatous eyes: evaluation of a causal relationship between the natural lens and open-angle glaucoma. *J Cataract Refract Surg*. 2009;35:1946–1955.
67. Johnstone MA. The aqueous outflow system as a mechanical pump: evidence from examination of tissue and aqueous movement in human and non-human primates. *J Glaucoma*. 2004;13:421–438.
68. Wang N, Chintala SK, Fini ME, Schuman JS. Ultrasound activates the TM ELAM-1/IL-1/NF-kappaB response: a potential mechanism for intraocular pressure reduction after phacoemulsification. *Invest Ophthalmol Vis Sci*. 2003;44: 1977–1981.
69. Benoist d'Azy C, Pereira B, Chiambaretta F, Dutheil F. Oxidative and anti-oxidative stress markers in chronic glaucoma: a systematic review and meta-analysis. *PLoS One*. 2016;11:e0166915.
70. Ferreira SM, Lerner SF, Brunzini R, Evelson PA, Llesuy SF. Antioxidant status in the aqueous humour of patients with

Investigative Ophthalmology & Visual Science

glaucoma associated with exfoliation syndrome. *Eye (Lond)*. 2009;23:1691–1697.

71. Ferreira SM, Lerner SF, Brunzini R, Reides CG, Evelson PA, Llesuy SF. Time course changes of oxidative stress markers in a rat experimental glaucoma model. *Invest Ophthalmol Vis Sci*. 2010;51:4635–4640.
72. Wang N, Chintala SK, Fini ME, Schuman JS. Activation of a tissue-specific stress response in the aqueous outflow pathway of the eye defines the glaucoma disease phenotype. *Nat Med*. 2001;7:304–309.
73. Tomarev SI. Eyeing a new route along an old pathway. *Nat Med*. 2001;7:294–295.
74. Wallace DM, Murphy-Ullrich JE, Downs JC, O'Brien CJ. The role of matricellular proteins in glaucoma. *Matrix Biol*. 2014; 37:174–182.
75. Izzotti A, Sacca SC, Longobardi M, Cartiglia C. Sensitivity of ocular anterior chamber tissues to oxidative damage and its relevance to the pathogenesis of glaucoma. *Invest Ophthalmol Vis Sci*. 2009;50:5251–5258.

Investigative Ophthalmology & Visual Science